High-spin states in^{65}Ga and possible triaxial structure

de Lima, A.P.; Hamilton, J.H.; Kawakami, H.; Kim, H.J.; Peker, L.K.; Ramayya, A.V.; Robinson, R.L.; Ronningen, R.M.

published in
Physical Review C
1980

document version
Publisher's PDF, also known as Version of record

PHYSICAL REVIEW C VOLUME 21, NUMBER 4 APRIL 1980

High-spin states in ^{65}Ga and possible triaxial structure

H. Kawakami,* A. P. de Lima,† R. M. Ronningen,‡ A. V. Ramayya, and J. H. Hamilton
Physics Department, Vanderbilt University, Nashville, Tennessee 37235

R. L. Robinson and H. J. Kim
Oak Ridge National Laboratory, Oak Ridge, Tennessee 37830

L. K. Peker
Natuurkundig Laboratorium der Vrije Universiteit, Amsterdam, Netherlands and NNDC, Brookhaven National Laboratory, Upton, New York 11796

(Received 29 October 1979)

Level structure of ^{65}Ga was investigated by in-beam γ-ray spectroscopy. Excitation function, γ-ray angular distribution, and γ-γ coincidence measurements were performed. From γ-ray energies and intensities and γ-γ coincidence relations, eleven new excited states were established and parities and spins up to $21/2^+$ were assigned. Bands of levels built on $f_{5/2}$ and $g_{9/2}$ orbitals were observed with spacings that suggest triaxial structure.

[NUCLEAR STRUCTURE ^{58}Ni(^{12}C, αp) $E=39$ MeV, ^{60}Ni(^{7}Li, $2n$) $E=18$–21 MeV; measured I_γ, E_γ, $I_\gamma(\theta)$, $\gamma\gamma_{\text{coin}}$, $\gamma\gamma_{\text{DCO}}$, I_γ (Ex. $E_{^7\text{Li}}$); deduced ^{65}Ga levels, J, π, γ multipolarity.]

I. INTRODUCTION

In-beam gamma-ray spectroscopy following heavy-ion reactions is particularly fruitful in identifying high-spin states and the bands to which these states belong. Such information can provide significant insight into the structure of the nucleus. In this study of high-spin levels in ^{65}Ga, we have identified states up to $\frac{21}{2}^+$; many of the levels can be grouped into bands built on states with spin-parities of $\frac{3}{2}^-$, $\frac{5}{2}^-$, and $\frac{9}{2}^+$. The properties of these bands suggest that triaxial deformation may occur in ^{65}Ga. A preliminary report of this work has appeared.[1]

Information on the low-lying levels of ^{65}Ga was already available from the reactions ^{64}Zn(^{3}He,d) (Ref. 2) and ^{64}Zn(d,n),[3] from the radioactive decay[4] of ^{65}Ge($T_{1/2}=1.5$ min) and from in-beam γ-ray spectroscopy.[5,6] Some theoretical studies also have been reported based on the particle-phonon coupling model.[7,8] The theoretical works are successfully applied to low-lying and low-spin states up to $\frac{9}{2}^-$. A $\frac{9}{2}^+$ state at 2.034 MeV was reported in the transfer reaction studies ^{64}Zn(d,n)^{65}Ga with a large spectroscopic strength[3] and is supported by in-beam γ-ray spectroscopy with α particles.[5] This level is assigned to the single particle $g_{9/2}$ orbit, which has been reported to play a very important role in this mass region.[9-11] Indeed, we find not only a band built on this orbital but also an interruption of that band by a $\frac{21}{2}^+$ level that is interpreted as having a $(g_{9/2})^3$ configuration.

II. EXPERIMENTAL PROCEDURE

The main experiments were made with the ^{58}Ni(^{12}C, αp)^{65}Ga reaction. Since in that reaction some γ rays were complex and some angular distributions were disturbed by the β decay of ^{65}Ge($T_{1/2}=1.5$ m) produced by the ^{58}Ni(^{12}C, αn) reaction, complementary data were obtained by the study of the ^{60}Ni(^{7}Li, $2n$) reaction. The targets, reactions, and measurements are summarized in Table I. The enriched ^{58}Ni target of thickness 0.72 mg/cm^2 was evaporated onto a Pt backing and the enriched ^{60}Ni target onto an Ni backing. The beams of ^{12}C and ^{7}Li were obtained from the EN tandem accelerator at ORNL. In the angular distribution measurements, γ rays were detected with two Ge(Li) detectors with energy resolution of 2.5 keV at 1.33 MeV. One detector was fixed at 90° and served as a monitor. The other was placed at angles of 0°, 55°, and 90° relative to the beam direction. As an additional check on Doppler broadening, we also measured the spectra at 150°. The distances between target and detectors were 15 cm. In the γ-γ coincidence measurements, the detectors were set at 0° and 90°. This choice of angles allows one to obtain angular correlation information from the expression

$$R=\frac{W(0°,90°)}{W(90°,0°)},$$

where the two angles are for the first and second member of a γ-ray cascade. This has been re-

TABLE I. Summary of the experiments.

Target	Reaction	Beam energy (MeV)	Measurement
^{58}Ni	^{58}Ni(^{12}C, αp)	39	$\gamma(\theta)$, γ-γ coin.
^{60}Ni	^{60}Ni(^{7}Li, $2n$)	18, 19, 20, and 21	$\gamma(E)$
^{60}Ni	^{60}Ni(^{7}Li, $2n$)	20	$\gamma(\theta)$

ferred to as directional correlation from oriented nuclei (DCO). The detector-target distances were 7 cm. The 1000×1000 coincidence events were stored in the CDC 3200 computer through a PDP-11 buffer memory. An RaE source was used for energy and efficiency calibrations.

III. ANALYSIS AND RESULTS

A. Level scheme

The singles γ-ray spectrum obtained from ^{58}Ni + ^{12}C is shown in Fig. 1. Spectra were analyzed with the KEI-11EF code (the fitting function is a Gaussian peak + exponential tail, and that of the background is arctangent + linear), developed by Komura,[12] and by hand for some peaks. The relative intensities and angular distributions are listed in Table II. The 750.0-, 919.1-, 1027.1-, 1075.2-, and 1096.3-keV γ rays are doublets in the ^{12}C induced reactions. One member of each doublet is produced by the ^{58}Ni(^{12}C, αp) reaction and the other by the ^{58}Ni(^{12}C, $2p$) reaction. Thus, the usefulness of the angular distribution data of these complex γ rays in these reactions may be limited. However, the main components in the 750.0-, 1027.1-, and 1096.3-keV γ rays are in ^{65}Ga. The 424.3-, 667.5-, 1034.2-, 1067.9-, 1135.4-, 1180.1-, and 1330.7-keV γ rays were only observed in coincidence spectra, so no A_2 and A_4 values could be extracted for these. The angular distribution of the 190.6-keV γ ray was disturbed by the thick target holder. Angular dis-

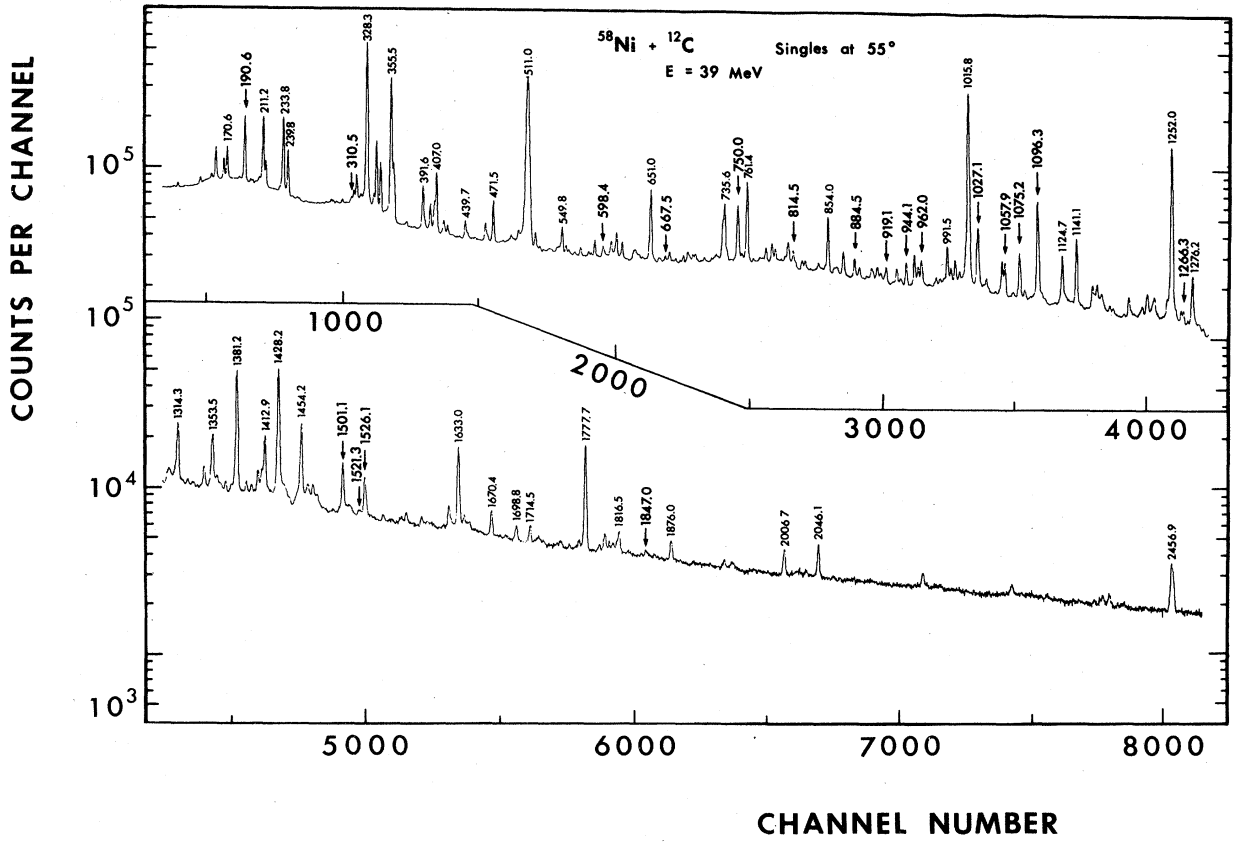

FIG. 1. The singles γ-ray spectra obtained from the ^{58}Ni + ^{12}C reaction at 55°. The γ rays in ^{65}Ga are marked by large numbers with an arrow. The other energy values are given for only strong γ rays.

TABLE II. Energies, intensities, and angular distributions of γ rays in ^{65}Ga.

E_γ (keV)	I_γ ^{12}C (39 MeV)	I_γ ^{7}Li (20 MeV)	A_2 ^{12}C (39 MeV)	A_4 ^{12}C (39 MeV)	A_2 ^{7}Li (20 MeV)	A_4 ^{7}Li (20 MeV)
190.6 (2)	100	100			−0.166 (12)	0.001 (12)
310.5 (2)	3.2 (4)	1.7 (3)	0.348 (38)	−0.002 (42)	0.43 (15)	0.04 (16)
424.3 (4)	0.5 (2)	0.5 (2)				
598.4 (5)	0.2 (1)	doublet	0.357 (38)	0.148 (37)		
667.5 (3)	3 (1)	3.8 (5)			−0.24 (12)	0.09 (14)
750.0 (5)	42 (4) [a]	27 (2)	[0.21 (5)	0.02 (6)] [a]	0.238 (31)	−0.036 (34)
814.5 (2)	9 (1)	3.4 (4)	0.304 (37)	−0.109 (41)	0.36 (11)	−0.05 (11)
884.5 (2)	14 (2)	14 (2)	−0.355 (25)	0.082 (29)	−0.308 (28)	0.070 (30)
919.1 (7)	13 (4) [a]	2.5 (3)			−0.11 (15)	0.03 (17)
944.1 (3)	12 (2)	10.1 (6)	−0.181 (30)	−0.038 (33)	−0.172 (25)	0.015 (30)
962.0 (3)	17 (2)	12 (2)	−0.39 (6)	0.05 (6)	−0.27 (7)	−0.03 (7)
1027.1 (2)	43 (4) [a]	22 (2)	[0.28 (6)	−0.06 (6)] [a]	0.35 (9)	−0.06 (8)
1034.2 (7)	2.0 (2)	weak				
1057.9 (3)	20 (2)	12 (2)	0.28 (6)	−0.08 (6)	0.233 (30)	−0.029 (34)
1067.9 (7)	3.2 (4)	weak				
1075.2 (5)	34 (2) [a]	18 (2)			0.350 (25)	−0.105 (30)
1096.3 (4)	68 (7) [a]	76 (5)	[0.295 (28)	−0.037 (25)] [a]	0.313 (24)	−0.047 (26)
1135.4 (7)	0.9 (3)	doublet				
1180.1	0.8 (3)					
1266.3 (8)	11 (2)	3.2 (5)	0.34 (22)	0.20 (28)		
1330.7 (7)	1.4 (4)	doublet				
1501.1 (5)	19 (2)	17 (2)	0.35 (8)	−0.16 (10)	0.39 (4)	−0.14 (5)
1521.3 (5)	1.8 (5)	3.5 (7)			−0.40 (10)	0.25 (9)
1526.1 (6)	9 (2)	10 (1)	−0.184 (44)	−0.02 (52)	−0.26 (8)	0.03 (7)
1847.0 (9)	1.1 (3)	2.3 (3)	0.44 (15)	0.14 (16)		

[a] Doublet with γ ray in ^{68}Ge.

tribution data obtained from the ^{60}Ni + ^{7}Li reaction were free of many of the above problems and so complemented the data from the ^{58}Ni + ^{12}C reaction. All the γ rays, except for those at 190.6, 750.0, 884.5, 962.0, 1075.2, 1096.3, 1135.4, and 1180.1 keV, are newly found in this experiment.

A typical coincidence spectrum is shown in Fig. 2. The 511.0–190.6 keV coincidence relation shows that the ^{65}Ga levels also were populated by the β decay of ^{65}Ge produced by the ^{58}Ni(^{12}C, αn) reaction. This fact was confirmed by the measurement of radioactivity with the beam off. The angular distributions of the 884.5- and 1075.2-keV transitions also were perturbed by the β-decay components.

The level scheme of ^{65}Ga based on our γ-ray energies, relative intensities, and coincidence relations is shown in Fig. 3. The already established low-lying states including their spins in

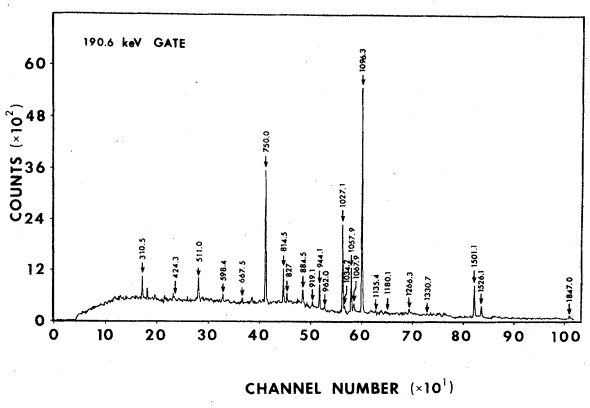

FIG. 2. The coincidence γ-ray spectra gated with the 190.6-keV γ ray.

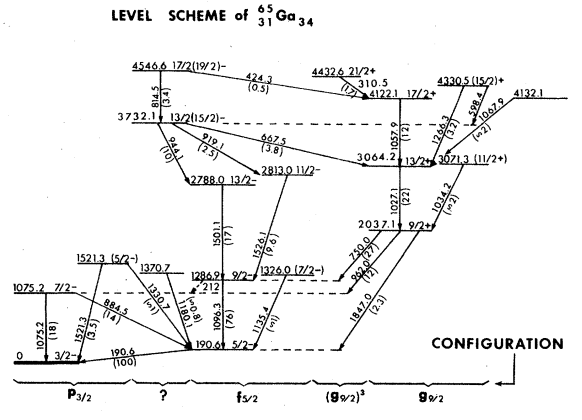

FIG. 3. The level scheme of ^{65}Ga obtained in the present experiment. The γ-ray intensities are obtained from the ^{60}Ni + ^{12}C reaction. The spin-parity assignments and groupings are described in Secs. III B and IV.

brackets, 190.6 [$\frac{5}{2}^-$], 1075.2 [$\frac{7}{2}^-$], 1286.9 [$\frac{9}{2}^-$], and 2037.1 [$\frac{9}{2}^-$] keV, are confirmed by the present data. The spin-parity assignments are described in Sec. III B, and the grouping of levels is explained in Sec. IV. The γ-ray relative intensities obtained from the ^{60}Ni and ^{7}Li (20 MeV) reaction are given in parentheses in Fig. 3.

B. Spin-parity assignments

Spins and parities are already established for the following levels by the radioactive decay studies,[4] reaction experiments,[2,3] and in-beam studies[5,6]: 0 keV, $\frac{3}{2}^-$; 190.6 keV, $\frac{5}{2}^-$; 1075.2 keV, $\frac{7}{2}^-$; 1286.9 keV, $\frac{9}{2}^-$; and 2037.1 keV, $\frac{9}{2}^+$. Our data are consistent with these assignments. Using these spins and parities, we assigned the spins and parities for other states based on our experimental DCO ratios and angular distribution data.

From our coincidence data we can deduce the following two primary cascades in the level scheme of ^{65}Ga: (1) 0←190.6←1096.3←1501.7←944.1←814.5 keV cascade and (2) 0←190.6←1096.3←750.0←1027.1←1507.9←310.5 keV cascade. The strong channel in the reaction of ^{12}C on ^{58}Ni is $2p$, that produces the levels in ^{68}Ge. The γ rays in ^{65}Ga have energies almost equal to those in ^{68}Ge. The interference of these γ rays made difficult an accurate analysis of the angular distribution data for the above cascades in ^{65}Ga. For this reason, we used DCO ratios for some γ rays to assign spins and parities and checked the assignments for consistency with the angular distribution data. The procedures for assigning spin-parities are outlined in the following six steps:

(1) The DCO ratio for a cascade of two stretched $E2$ transitions = 1, independent of attenuation coefficients α_2 and α_4. From the DCO ratios of $\simeq 1$ as given in Table III for the pairs (1501.1-1096.3 keV), (750.0-1027.1 keV), (1027.1-1057.9 keV), (1057.9-310.5 keV), we assigned spins and parities to the levels at 2788.0 keV, $\frac{13}{2}^-$; 3064.2 keV, $\frac{13}{2}^+$; 4122.1 keV, $\frac{17}{2}^+$; and 4432.6 keV, $\frac{21}{2}^+$. Our angular distribution data for transitions from the above levels are consistent with the fact that for a stretched $E2$ transition the angular distribution coefficients $A_2 \simeq 0.25-0.35$ and $A_4 \simeq -0.1$ (see Table IV).

(2) The experimental DCO ratio of the 1096–191 keV cascade (note that the efficiency corrections were measured for both detectors) is 0.25 ± 0.03.

TABLE III. Comparison of the experimental DCO ratio with those calculated for the listed spin sequences and δ values. Errors are shown in parentheses.

$\gamma_1 \rightarrow \gamma_2$	DCO ratio Experiment	DCO ratio Theory	Spin seq. and multipolarity I_1	$(L_1(\delta_1)L_1')$	I_2	$(L_2(\delta_2)L_2')$	I_3	Mixing ratio[a] $\delta_1 = \frac{\langle \vert L+1 \vert \rangle}{\langle \vert L \vert \rangle}$	Mixing ratio[a] $\delta_2 = \frac{\langle \vert L+1 \vert \rangle}{\langle \vert L \vert \rangle}$
884 → 190	0.87 (15)	0.81	$\frac{7}{2}^-$	(D, Q)	$\frac{5}{2}^-$	(D, Q)	$\frac{3}{2}^-$	−0.23 (4)	−0.7
1096 → 190	0.25 (3)	0.25	$\frac{9}{2}^-$	(Q, D)	$\frac{5}{2}^-$	(D, Q)	$\frac{3}{2}^-$		−0.7 (3)
1847 → 190	0.45 (25)	0.23	$\frac{9}{2}^+$	(Q, Q)	$\frac{5}{2}^-$	(D, Q)	$\frac{3}{2}^-$		−0.7
962 → 884	1.6 (11)	0.78	$\frac{9}{2}^+$	(D, Q)	$\frac{7}{2}^-$	(D, Q)	$\frac{5}{2}^-$	−0.10	−0.23
962 → 1075	2.0 (6)	2.56	$\frac{9}{2}^+$	(D, Q)	$\frac{7}{2}^-$	(Q, Q)	$\frac{3}{2}^-$	−0.10 (5)	
750 → 1096	0.97 (13)	0.95	$\frac{9}{2}^+$	(D, Q)	$\frac{9}{2}^-$	(Q, Q)	$\frac{5}{2}^-$	0 (≥ −0.2)	
1501 → 1096	0.92 (21)	1.00	$\frac{13}{2}^-$	(Q, Q)	$\frac{9}{2}^-$	(Q, Q)	$\frac{5}{2}^-$		
1526 → 1096	2.5 (8)	2.0	$\frac{11}{2}^-$	(D, Q)	$\frac{9}{2}^-$	(Q, Q)	$\frac{5}{2}^-$	0 (0.04)	
944 → 1501	2.4 (4)	2.4	$\frac{13}{2}^-$	(D, Q)	$\frac{13}{2}^-$	(Q, Q)	$\frac{9}{2}^-$	−1.4 (~10)	
919 → 1526	0.5 (3)	0.5	$\frac{13}{2}^-$	(D, Q)	$\frac{11}{2}^-$	(Q, Q)	$\frac{9}{2}^-$	0.3 (>0.1)	
814 → 944	0.50 (14)	0.37	$\frac{17}{2}^-$	(Q, Q)	$\frac{13}{2}^-$	(D, Q)	$\frac{13}{2}^-$		−1.4
1027 → 750	0.93 (13)	1.05	$\frac{13}{2}^+$	(Q, Q)	$\frac{9}{2}^+$	(D, Q)	$\frac{9}{2}^-$		0
1027 → 962	0.24 (14)	0.35	$\frac{13}{2}^+$	(Q, Q)	$\frac{9}{2}^+$	(D, Q)	$\frac{7}{2}^-$		−0.10
1058 → 1027	0.98 (12)	1.00	$\frac{17}{2}^+$	(Q, Q)	$\frac{13}{2}^+$	(Q, Q)	$\frac{9}{2}^+$		
1266 → 1027	0.5 (3)	0.76	$\frac{15}{2}^+$	(D, Q)	$\frac{13}{2}^+$	(Q, Q)	$\frac{9}{2}^+$	0.6 (1)	
		or 0.73						or 2.3 (5)	
310 → 1058	0.9 (4)	1.00	$\frac{21}{2}^+$	(Q, Q)	$\frac{17}{2}^+$	(Q, Q)	$\frac{13}{2}^+$		

[a]These values are either obtained from angular distribution data or DCO ratios consistent with α_2 and α_4 values.

TABLE IV. Experimental and calculated A_2 and A_4 values (^{12}C, 39 MeV) are compared.

E_γ in keV	A_2 Exp.	A_2 Cal.	A_4 Exp.	A_4 Cal.
190.6		−0.554		0.028
310.5	0.348 (38)	0.352	−0.002 (42)	−0.102
598.4	0.357 (38)	0.324	0.148 (37)	−0.005
750.0	[0.21 (5)] [a]	0.299	[0.02 (6)] [a]	−0.000
814.5	0.304 (37)	0.334	−0.109 (41)	−0.085
884.5	−0.355 (25)	−0.360	0.082 (29)	0.004
944.1	−0.181 (30)	−0.198	−0.038 (33)	−0.129
962.0	−0.39 (6)	−0.330	0.05 (6)	0.001
1027.1	[0.28 (6)] [a]	0.323	[−0.06 (6)] [a]	−0.081
1057.9	0.28 (6)	0.338	−0.08 (6)	−0.092
1096.3	[0.295 (28)] [a]	0.280	[−0.037 (25)] [a]	−0.054
1266.3	0.34 (22)	0.48	0.20 (28)	0.08
1501.1	0.35 (8)	0.302	−0.16 (10)	−0.065
1526.1	−0.184 (44)	−0.196	−0.02 (5)	−0.000
1847.0	0.44 (15)	0.29	0.14 (16)	−0.06

[a] Doublet with a γ ray in ^{68}Ge.

This value is consistent with the known spin sequence of $\frac{9}{2}^- \rightarrow \frac{5}{2}^- \rightarrow \frac{3}{2}^-$ if we assume the attenuation coefficient $\alpha_2 \geq 0.60$ for the 1286.9-keV state. This is illustrated in Fig. 4. The DCO ratio yields $\delta = (E2/M1)^{1/2} = -0.7 \pm 0.3$ for the 190.6-keV transition if α_2 is taken as 0.60. We assumed this attenuation coefficient for the 1286.9-keV level, even though it allows a possibility of $33^{+17}_{-19}\%$ $E2$ admixture in the $\frac{5}{2}^- \rightarrow \frac{3}{2}^-$ 190.6-keV transition, because a larger α_2 value, which would yield a smaller δ as might be expected from systematics, is not reasonable for such a low-lying $\frac{9}{2}^-$ state. (A larger α_2 value would not be consistent with the α's for the higher-spin states either.) In order to be able to assign spins and parities to other levels from DCO ratio one should have knowledge of α_2 and α_4 for various states. The procedures for obtaining consistent α_2 and α_4 are discussed in steps 3 and 4 below.

(3) After steps 1 and 2, we obtained α_2 values for the 2037.1-, 2788.0-, and 3064.2-keV levels from the DCO ratios (R) of the following coincidence pairs: R(750 → ( ) → 191-keV) = 0.24 ± 0.02; R(1501 → ( ) → 191-keV) = 0.21 ± 0.05; R(1027 → ( ) → ( ) → 190-keV) = 0.22 ± 0.06. An example of the relation between R and α_2 is illustrated on the left of Fig. 5 for the 1027–191 keV cascade. This is calculated for $\delta_{191} = 0.7$ and yields $\alpha_2 = 0.75 \pm 0.10$ for the 3064-keV state. The dependence of R on δ_{191} is illustrated on the right of Fig. 5. Inclusion

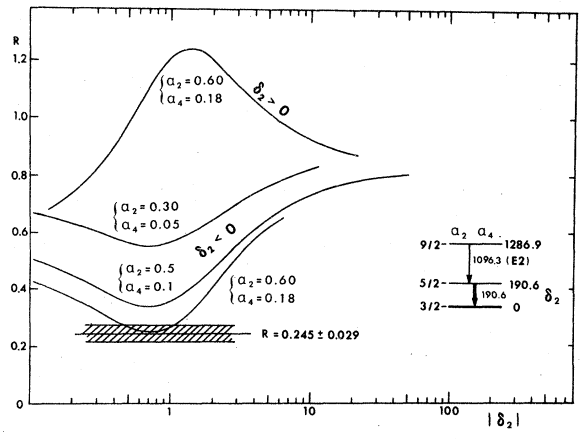

FIG. 4. The DCO ratio of the 1096.3–190.6-keV γ-ray cascade. Parameters are the attenuation coefficients α_2 and α_4 of the 1286.9-keV, $\frac{9}{2}^-$ state.

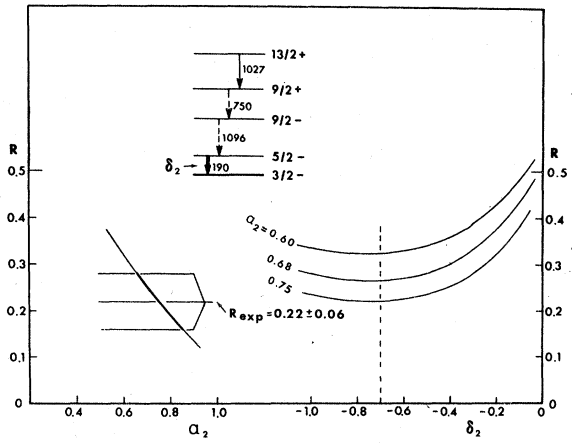

FIG. 5. The DCO ratio of the 1026–190.6-keV γ-ray cascade with the two intermediate transitions of 750 and 1096 keV unobserved (a skipped correlatiion). The experimental α_2 value obtained was 0.75 ± 0.10. The details are given in the text.

of the error in $\delta_{191}(0.7 \pm 0.3)$ raises the error on α_2 to ± 0.14. This result is consistent with the value of 0.79 ± 0.20 obtained independently from the analysis of the 1027-keV γ-ray angular distribution. The experimental α_2 values obtained for the levels mentioned above by this method are shown in column 3 of Table V.

(4) We estimated the α_2 values for the other states with the following two assumptions: (1) The population of the nuclear substates is Gaussian, and (2) the parameter σ which defines the width of the Gaussian (see Ref. 13 for the definition of σ) is the same for all spins. Calculated α_2 values are shown in Fig. 6 for various states. The curve marked "CASCADE" is an example for a cascade beginning at a state with $J = \frac{21}{2}$ and $\alpha_2 = 0.88$. When a side-feeding curve for $\sigma = 2.25$ is added to the cascade-feeding curve, the α_2 values are consistent with the experimental ones obtained from DCO ratios in step 3. Also shown in Fig. 6 is the curve for the variation of α_2 with J for 100% side-feeding transitions with $\sigma = 2.25$. For higher-spin states, which are populated only by side feedings, such as the 4330.5-keV level, the α_2 values are obtained from the curve for side feeding with $\sigma = 2.25$. For a state of lower spin J, the α_2 values are obtained by taking the weighted mean

$$\alpha_2(J) = \frac{\alpha_{2c}(J')\,U(J' \to J)\,I_c + \alpha_{2s}(J)\,I_s}{I_c + I_s},$$

where $U(J' \to J)$ is the attenuation by a cascade transition (the values are tabulated in Ref. 13), $\alpha_{2c}(J')$ is the known α_2 of the higher-lying J' state which depopulates to the J state, and $\alpha_2(J)$ is the value from the side-feeding curve as shown in Fig. 6. Here I_c and I_s are the relative intensities of cascade feeding and side feeding. From this calculation, we obtain 0.57 for the α_2 value of the 1286.9-keV, $\frac{9}{2}^-$ state. This value is in good agreement with 0.60 in step 2. The calculated α_2 values are listed in Table V. These values are in excellent agreement with the experimental values obtained from DCO ratios, as shown in Table V and in Fig. 6. The α_2 values in the parentheses in Table V are the values for the case of the less likely $\frac{15}{2}^-$ and $\frac{19}{2}^-$ assignments for the 3732.1 and 4546.6-keV states, respectively. The α_4 values are determined from the α_2 values by assuming a Gaussian distribution.

(5) Using the α_2 and α_4 values from step 4, we calculated the DCO ratios, which compare very well with the experimental values, as given in Table III. The calculated values of A_2 and A_4 for each spin assignment also are in very good agreement with the experimental ones and thus support the spin assignments.

(6) The γ-ray yield curves obtained from the $^{60}\mathrm{Ni} + ^{7}\mathrm{Li}$ experiment are illustrated in Fig. 7, together with the spin-parity assignments from the above. Black points are for the positive parity states and the open circles are for the negative parity states. The yield curve for each successively higher-spin state increases more steeply with the projectile energy than the curve for the lower-

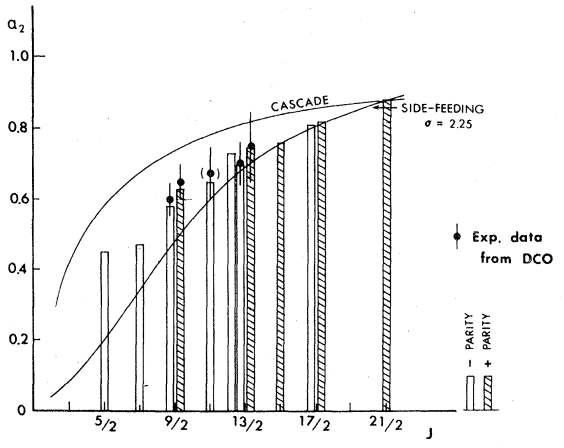

FIG. 6. Calculated α_2 for even-parity (shaded columns) and odd-parity (open columns) states are shown. Details for the calculations are given in the text.

TABLE V. The attenuation coefficients used in the present analysis. The calculated values are for the less likely spin assignments shown in parentheses for the 3732.1- and 4546.6-keV levels. "Exp. Data" means the values obtained from the experimental DCO ratio. "Calculated" means the calculated values that reproduce the angular distribution data.

State (keV)	Spin	Attenuation coefficients α_2 Exp. Data	Calculated
190.6	$\frac{5}{2}^-$		0.45
1075.2	$\frac{7}{2}^-$		0.47
1286.9	$\frac{9}{2}^-$	0.60[a]	0.57
2037.1	$\frac{9}{2}^+$	0.65 ± 0.07	0.63
2788.0	$\frac{13}{2}^-$	0.71 ± 0.08	0.70 (0.75)
2813.0	$\frac{11}{2}^-$		0.63 (0.65)
3064.2	$\frac{13}{2}^+$	0.75 ± 0.14	0.75 (0.76)
3732.1	$\frac{13}{2}$ $(\frac{15}{2}^-)$		0.73 (0.80)
4122.1	$\frac{17}{2}^+$		0.82 (0.82)
4330.5	$\frac{15}{2}^+$		0.76
4432.6	$\frac{21}{2}^+$		0.88
4546.6	$\frac{17}{2}^-$ $(\frac{19}{2}^-)$		0.81 (0.85)

[a]Assumed value (see text for clarification).

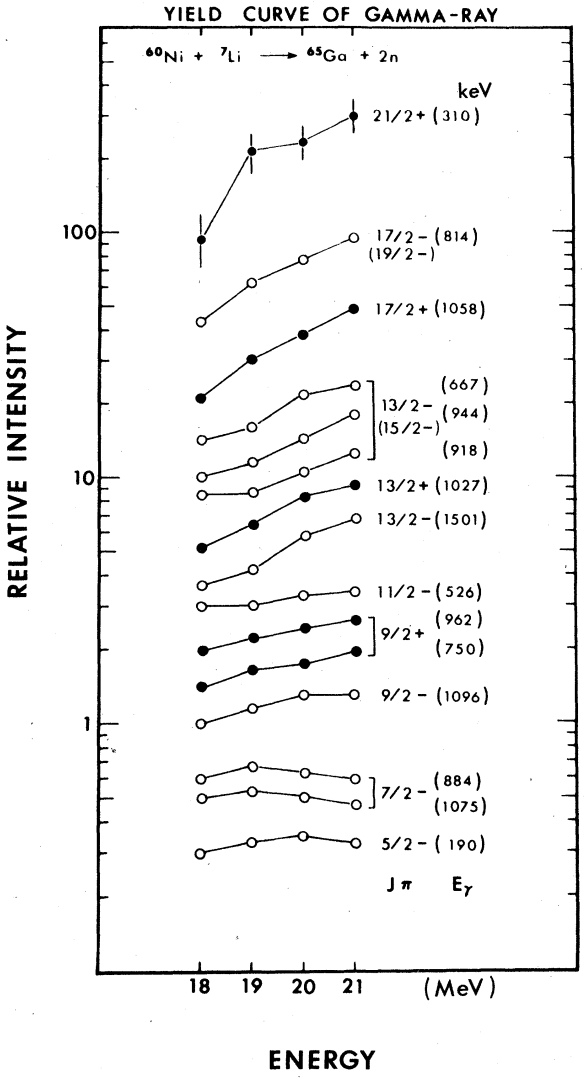

FIG. 7. The γ-ray yield curve obtained from the ^{60}Ni+^{7}Li reaction. The spin-parities assigned in Sec. III B are also given.

spin state just below it. In every case, the spin assignments based on the slope of the yield curves with increase in projectile energy are consistent with the assignments extracted from steps (1)–(5). These yield curves provide independent evidence to help rule out choices that are allowed within two standard deviations, for example, by A_2, A_4, and R.

The spins and parities as deduced in the above ways are shown in the level scheme in Fig. 3. The spin-parity assignments deduced from the different procedures are given in Table VI. The spins and parities are shown in parentheses in Fig. 3 when the data favor but do not uniquely establish them. For the 3732.1 and 4546.6 keV levels, assignments which are allowed but also less favored are shown in parentheses.

C. Mean life measurements

A Doppler shift was definitely observed only for the 1501-keV γ ray in ^{65}Ga. The mean life extracted from the Doppler shift for the 2788.0-keV, $\frac{13}{2}^-$ state was 0.8± 0.4 ps. The data were analyzed with the DOPCO program.

IV. DISCUSSION

The specific features of interest in the ^{65}Ga level scheme obtained in the present experiment are as follows:

(a) $E2$ transitions with strong intensities are observed as the first transition in each band ($\frac{7}{2}^- \rightarrow \frac{3}{2}^-$, $\frac{9}{2}^- \rightarrow \frac{5}{2}^-$, and $\frac{13}{2}^+ \rightarrow \frac{9}{2}^+$) and in each case the transition energy is nearly the same.

(b) Other strong $E2$ transitions observed are those terminating at the $\frac{9}{2}^-$, 1287-keV, and $\frac{13}{2}^+$, 3064-keV, states.

(c) Besides the spin sequences of $J+4 \rightarrow J+2 \rightarrow J$, the spin sequences $J+3 \rightarrow J+2 \rightarrow J$ are also detected, for example, the sequences $\frac{11}{2}^- \rightarrow \frac{9}{2}^- \rightarrow \frac{5}{2}^-$ and $\frac{15}{2}^+ \rightarrow \frac{13}{2}^+ \rightarrow \frac{9}{2}^+$.

(d) The energy of the transition from the $\frac{21}{2}^+$ to the $\frac{17}{2}^+$ state is very small in comparison to the other stretched $E2$ transition energies in the cascade.

The shell model orbits in this mass region are $p_{3/2}$, $f_{5/2}$, $p_{1/2}$, and $g_{9/2}$. The shell model states identified from the transfer reaction experiment[3] are the $p_{3/2}$ ground state; the $f_{5/2}$ level at 190.6-keV level and $g_{9/2}$ level at 2037.1 keV. The error on the $E2$ mixing ratio $\delta(E2/M1) = -0.7 \pm 0.3$ of the 190.6-keV $f_{5/2} \rightarrow p_{3/2}$ transition is sufficiently large that one cannot say for certain whether it is near zero or near one. A large value may be reasonable because the $M1$ decay is l forbidden. Note in the decay of the $g_{9/2}$ state at 2037.1 keV, the 1847.0-keV transition is consistent with pure $M2$ and the 962.0-keV transition may have a small admixture (99% $E1$ + 1% $M2$), as shown in Table III. The $M2$ mixing shows that the $E1$ transitions from the $g_{9/2}$ state to the $f_{5/2}$ band are relatively retarded in comparison to shell model prediction.

The low-spin $p_{1/2}$ state was not observed in the heavy-ion induced reactions which transfer large angular momenta. A $\frac{1}{2}^-$ state, however, has been reported at 62 keV in radioactive decay studies[4] and in a reaction experiment.[3] The 62-keV, $\frac{1}{2}^-$ state is probably a $p_{1/2}$ quasiparticle state.[3]

The evidence noted in point (a) above for the $J+2$ states at 1075.2 keV, $\frac{7}{2}^-$; 1286.9 keV, $\frac{9}{2}^-$; and 3064.2 keV, $\frac{13}{2}^+$ strongly suggests these states are

TABLE VI. Spin assignments to the levels in ^{65}Ga.

Level (keV)	E_γ (keV)	$\gamma(\theta)$ DCO	Yield curves	Decay mode	Expected from syst.	Previous assignments	Adopted J^π
190.6	190.6	$\frac{1}{2}, \frac{5}{2}$	$\frac{3}{2}-\frac{7}{2}$	$\frac{1}{2}-\frac{7}{2}$		$\frac{5}{2}^-$ (Refs. 2, 3, 5)	$\frac{5}{2}^-$
1075.2	884.5	$\frac{7}{2}^-$	$\frac{3}{2}-\frac{9}{2}$	$\frac{3}{2}-\frac{7}{2}$	$\frac{7}{2}^-$	$\frac{7}{2}^-$ (Ref. 5)	$\frac{7}{2}^-$
	1075.2						
1286.9	212	$\frac{9}{2}^-$	$\frac{5}{2}-\frac{11}{2}$	$\frac{5}{2}-\frac{9}{2}$	$\frac{9}{2}^-$	$\frac{9}{2}^-$ (Ref. 5)	$\frac{9}{2}^-$
	1096.3						
1326.0	1135.4			$\frac{1}{2}-\frac{9}{2}$	$\frac{5}{2}, \frac{7}{2}^-$		$(\frac{7}{2}^-)$
1370.7	1180.1			$\frac{1}{2}-\frac{9}{2}$		$(\frac{5}{2}^-)$ (Ref. 5)	$(\frac{5}{2}^-)$
1521.3	1521.3	$\frac{3}{2}, \frac{5}{2}$		$\frac{1}{2}-\frac{7}{2}$			$(\frac{5}{2}^-)$
	1330.7						
2037.1	750.0	$\frac{9}{2}^+$	$\frac{7}{2}-\frac{11}{2}$	$\frac{5}{2}-\frac{9}{2}$		$\frac{9}{2}^+$ (Refs. 2, 3, 5)	$\frac{9}{2}^+$
	962.0						
	1847.0						
2788.0	1501.1	$\frac{13}{2}^-$	$\frac{13}{2}, \frac{15}{2}$	$\frac{5}{2}-\frac{13}{2}$	$\frac{13}{2}^-$		$\frac{13}{2}^-$
2813.0	1526.1	$\frac{9}{2}, \frac{11}{2}$	$\frac{7}{2}-\frac{11}{2}$	$\frac{5}{2}-\frac{13}{2}$	$\frac{11}{2}, \frac{13}{2}^-$		$\frac{11}{2}^-$
3064.2	1027.1	$\frac{9}{2}, \frac{13}{2}^+$	$\frac{13}{2}-\frac{15}{2}$	$\frac{5}{2}-\frac{13}{2}$	$\frac{13}{2}^+$		$\frac{13}{2}^+$
3071.3	1034.2				$\frac{11}{2}^+$		$(\frac{11}{2}^+)$
3732.1	667.5	$\frac{13}{2}, \frac{15}{2}$	$\frac{11}{2}-\frac{15}{2}$	$\frac{9}{2}-\frac{15}{2}$			$\frac{13}{2}$ $(\frac{15}{2})$
	919.1						
	944.1						
4122.1	1057.9	$\frac{13}{2}, \frac{17}{2}$	$\geq\frac{15}{2}$	$\frac{9}{2}-\frac{17}{2}$	$\frac{17}{2}$		$\frac{17}{2}^+$
4132.1	1067.9						
4330.5	598.4	$(\frac{15}{2})$		$\frac{11}{2}-\frac{17}{2}$	$\frac{15}{2}-\frac{17}{2}$		$(\frac{15}{2}^+)$
	1266.3						
4432.6	310.5	$(\frac{21}{2})$	$\geq\frac{17}{2}$	$\frac{13}{2}-\frac{21}{2}$	$\frac{21}{2}$		$\frac{21}{2}^+$
4546.6	424.3	$\frac{17}{2}$ $(\frac{19}{2})$	$\geq\frac{13}{2}$	$\frac{13}{2}-\frac{19}{2}$	$\frac{17}{2}, \frac{19}{2}$		$\frac{17}{2}$ $(\frac{19}{2})$
	814.5						

formed through the coupling of the single quasiparticles in the $p_{3/2}$, $f_{5/2}$, and $g_{9/2}$ states, to the first 2^+ state of a neighboring even-even nucleus. The energies of the first excited 2^+ states, 991.5 and 957 keV for neighboring ^{64}Zn and ^{66}Ge, respectively, are very similar to the energies of the three $J+2\rightarrow J$ transitions. One then could expect that the $J+4$ states at 2788.0 keV, $\frac{13}{2}^-$ and 4122.1 keV, $\frac{17}{2}^+$ would fit the description of coupling of a single quasiparticle to the first 4^+ state of the even mass core. However, the energies of the $4^+\rightarrow 2^+$ transitions in the even-even neighbors are 1315.2 and 1217.9 keV for ^{64}Zn and ^{66}Ge, respectively. The differences between these energies and the $J+4\rightarrow J+2$ transition energies of 1057.9 and 1501.1 keV in ^{65}Ga indicate that the single particle + core coupling scheme in the framework of the weak coupling model is not so good for higher-spin states.

Another explanation for the $J+2\rightarrow J$ sequence that will also include the $J+1\rightarrow J$ sequence is that ^{65}Ga has a triaxial nuclear shape. In the special case of $\gamma=0°$, where γ is a measure of the asymmetry of the nucleus, the model reduces to the decoupling scheme described by Stephens.[14] Meyer-Ter-Vehn[15] has made predictions of the triaxial model in the $A=135$ and $A=190$ mass regions. Predictions of the model in the two extreme situations $\gamma=0°$ and 30° are given in Fig. 8. These predictions, which are based on the Davydov approximation,[16] were taken from Figs. 5(a) and 5(b) in Ref. 15, in which the case of the unique-parity state $j=\frac{11}{2}$ in $A=192$ is calculated. The important

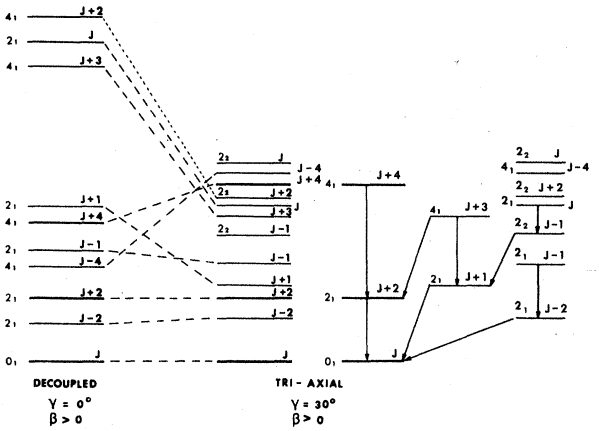

FIG. 8. The simplified level scheme for the decoupled scheme (the triaxial model with $\gamma = 0°$) and for the triaxial scheme ($\gamma = 30°$). The level scheme for $\gamma = 30°$ is rearranged on the right side; there, the solid lines between states represent the predicted strong $E2$ transitions. The numbers with subscripts are the states in the even-even core; for example, 4_1 means the first excited 4^+ state in the even-even core nucleus.

point is that, besides the $J+4 \rightarrow J+2 \rightarrow J$ sequence, the spin sequences of $J+1 \rightarrow J$, $J+3 \rightarrow J+2$, and so on are predicted in the triaxial model, as shown in the right side of Fig. 8. The energies of the $J+1$ and $J+3$ states are strongly influenced by the introduction of the asymmetry. These experimental spin sequences are not reproduced by the decoupled scheme based on axial symmetry. The solid lines between states represent the strong $E2$ transitions theoretically predicted. The relative positions of the $J+4$ and $J+3$ states depend on the γ value. From Ref. 15, the excited energy of the $J+4$ state is higher than that of the $J+3$ for $\gamma > 20°$, and vice versa for $\gamma < 20°$. Now consider the ^{65}Ga level scheme from the point of view of the triaxial model. The level spacing of the bands built on the assigned $f_{5/2}$ and $g_{9/2}$ states are similar and compare favorably to the predictions of the triaxial model. From the fact that the excitation energies of the $\frac{11}{2}^-$ and $\frac{15}{2}^-$ states are higher than that of the $\frac{13}{2}^-$ and $\frac{17}{2}^+$ states, respectively, the γ value is expected to be less than 20° in ^{65}Ga. A good candidate for the $J+1$ state for the $\frac{3}{2}^-$ band is seen at 1521.3 keV. While we could not definitely assign $J+1$ states in the $\frac{5}{2}^-$ and $\frac{9}{2}^+$ bands, we do observe candidates for these states at 1326.0 and 3071.3 keV. Besides that, we can expect some low-lying states with $J-2$ or $J-1$ spin, as shown in Fig. 8. Some low-lying spin states have been reported at 890 keV ($\frac{1}{2}^-$ or $\frac{3}{2}^-$),[4] 821 keV ($\frac{1}{2}^-$),[3] and 2822 or 2927 keV ($\frac{5}{2}^+$),[3] in other experiments. To evaluate more carefully the validity of the triaxial model, calculations need to be made in the $A = 70$ mass region. Further, the test should include a comparison of transition probabilities which are not known theoretically or experimentally.

The other interesting feature of ^{65}Ga is that mentioned in (d) above. The low energy 310.5 keV of the transition between the $\frac{21}{2}^+$ and $\frac{17}{2}^+$ states clearly indicates that the $\frac{21}{2}^+$ state has a different structure from the band built on the $\frac{9}{2}^+$ state at 2037.1 keV. Nearby even-even nuclei have 8^+ states in the energy range of 4.5–5 MeV, which have been interpreted as $(g_{9/2})^2$ configuration.[9] Since the lowest spin of a $(g_{9/2})^3$ configuration is $\frac{21}{2}^+$, we suggest that the state at 4432.6 keV may be such a three quasiparticle configuration.

At present we have no explanation for the remaining states at 1371, 3732, 4132, and 4547 keV. However, the spins of the 3732 and 4547 keV levels and their energy spacing suggest they are the first two members of a band.

ACKNOWLEDGMENTS

One of us (H.K.) would like to thank the Nuclear Physics group at Vanderbilt for their hospitality while he was staying at Vanderbilt. One of us (A.P.L.) is on fellowship from Instituto Nacional de Investigacao, Cientifica, Portugal. The program DOPCO used in the Doppler shift prediction was written by W. T. Milner of ORNL. This work was supported in part by a grant from the Department of Energy and sponsored in part by the Department of Energy under contract with the Union Carbide Corporation.

*Present address: Institute for Nuclear Study, University of Tokyo, Japan.
†Present address: Physics Dept., University of Coimbra, Portugal.
‡Present address: Physics Department, Michigan State University, East Lansing, Michigan.

[1] H. Kawakami, A. P. de Lima, J. H. Hamilton, R. M. Ronningen, A. V. Ramayya, R. L. Robinson, H. J. Kim, and L. K. Peker, in *Proceedings of the International Conference on Nuclear Structure, Tokyo*, 1977, edited by T. Marumori (Physical Society of Japan, Tokyo, 1978), p. 274.

[2]M. G. Betigeri, H. H. Duhm, R. Santo, R. Stock, and R. Bock, Nucl. Phys. A100, 416 (1967).
[3]R. G. Couch, J. A. Biggerstaff, F. G. Perey, S. Raman, and K. K. Seth, Phys. Rev. C 2, 149 (1970).
[4]H. W. Jongsma, J. C. de Lange, H. Verheul, FW. N. de Boer, and P. F. A. Goudsmit, Z. Phys. 262, 247 (1973).
[5]L. Harms-Rindahl, J. Sztarkier, and Z. P. Sawa, Phys. Scr. 9, 15 (1974).
[6]P. R. Chagnon, J. W. Mihelich, G. F. Neal, F. P. Venezia, R. L. West, and Z. P. Sawa, Annual Report of Research Institute of Physics, Stockholm, Sweden (1975).
[7]R. Almar, O. Civitarese, F. Krmpotic, and J. Navaza, Phys. Rev. C 6, 187 (1972).
[8]V. Paar, Nucl. Phys. A211, 29 (1973).
[9]A. P. de Lima, J. H. Hamilton, A. V. Ramayya, B. van Nooijen, R. M. Ronningen, H. Kawakami, R. B. Piercey, R. L. Robinson, H. J. Kim, W. K. Tuttle, L. K. Peker, F. A. Rickey, and R. Popli, Phys. Lett. 83B, 43 (1979).
[10]J. H. Hamilton, R. L. Robinson, and A. V. Ramayya, *Nuclear Interactions*, edited by B. A. Robson (Springer, New York, 1979), p. 253.
[11]G. F Neal, Z. P. Sawa, F. P. Venezia, and P. R. Chagnon, Nucl. Phys. A280, 161 (1977).
[12]K. Komura, Institute for Nuclear Study Report No. INS-TCH 9 (1974).
[13]T. Yamazaki, Nucl. Data A3, 1 (1967).
[14]F. S. Stephens, in *Proceedings of the International Conference on Nuclear Physics, Munich*, 1973, edited by J. de Bohr and H. J. Mang (North-Holland, Amsterdam, 1973), Vol. 2, p. 367.
[15]J. Meyer-Ter-Vehn, Nucl. Phys. A249, 111 (1975); A249, 141 (1975).
[16]A. S. Davydov and G. F. Filippov, Nucl. Phys. 8, 237 (1958); A. S. Davydov and V. S. Rostovsky, *ibid.* 12, 58 (1959).